

Particle Production within the Quark Meson Coupling Model

P.K. Panda

*Indian Association for the Cultivation of Science, Jadavpur, Kolkata-700 032, India and
Centro de Física Computacional, Department of Physics,
University of Coimbra, 3004-516 Coimbra, Portugal*

D.P.Menezes

Depto de Física - CFM - Universidade Federal de Santa Catarina Florianópolis - SC - CP. 476 - CEP 88.040 - 900 - Brazil

C. Providência

*Centro de Física Computacional, Department of Physics,
University of Coimbra, 3004-516 Coimbra, Portugal*

Quark meson coupling (QMC) models can be successfully applied to the description of compact star properties in nuclear astrophysics as well as to nuclear matter. In the regime of hot hadronic matter very few calculations exist using the QMC model, in particular when applied to particle yields in heavy ion collisions. In the present work, we identify the free energy of the bag with the effective mass of the baryons and we calculate the particle production yields on a Au+Au collision at RHIC with the QMC model and compare them with results obtained previously with other relativistic models. A smaller temperature for the fireball, $T=132$ MeV, is obtained due to the smaller effective baryon masses predicted by QMC. QMC was also applied to the description of particle yields at SPS in Pb+Pb collisions.

PACS number(s): 21.65.+f, 24.10.Jv, 95.30.Tg

I. INTRODUCTION

The knowledge of the equation of state (EoS) of nuclear matter under exotic conditions, including high isospin asymmetries, finite temperatures, and a wide density range, is essential for our understanding of the nuclear force. It is important to impose constraints coming both from laboratory measurements and astrophysical on the nuclear models presently used to describe nuclear matter.

The quark-gluon plasma (QGP) phase refers to matter where quarks and gluons are believed to be deconfined and it probably takes place at temperatures of the order of 150 to 170 MeV. These temperatures were possible in nature only shortly after the Big Bang. In large colliders around the world (RHIC/BNL, ALICE/CERN, GSI, etc), physicists are trying to convert hadronic matter at sufficiently high temperatures into QGP. Possible experiments towards this search are Au-Au collisions at RHIC/BNL and Pb-Pb collisions at SPS/CERN, where the hadron abundances and particle ratios are used in order to determine the temperature and baryonic chemical potential of the possibly present hadronic matter-QGP phase transition.

Recently relativistic nuclear models have been tested in the high temperature regime produced in these heavy ion collisions. In previous works these data have already been analyzed [1, 2, 3, 4, 5] under different perspectives. In [2] the authors have used a statistical model which assumes chemical equilibration to find the temperature and baryon chemical potential that provide a

best fit to the data obtained by the NA49 [6] and WA97 [7] collaborations. In this work the interaction among the baryons and mesons were neglected and an eigenvolume was assigned to all particles so that repulsive interactions among hadrons were considered. In [3] the nuclear interaction was included through a relativistic self-consistent chiral model of hadrons, which embodies the restoration of chiral symmetry at both high temperatures and densities. The results depended on the parametrizations used and indicated that no direct freeze-out from the restored phase was observed.

In [4] four parametrizations of the non-linear Walecka model [8], namely NL3 [9], TM1 [10], GM1 and GM3 [11], one model with implicit density dependence through meson field couplings, the $NL\omega\rho$ [12] and two different parametrizations of a density dependent hadronic model, the TW [13] and the DDME1 [14] were used to calculate the Au-Au collision particle yields. Eighteen baryons, 3 mesons to mediate the nuclear force and pions, kaons, ρ s and K^* s were included. It was shown that if the light mesons, e.g. pions and kaons, are not taken in the interaction with baryons the models do not have enough repulsion among hadrons and are not able to reproduce experimental data with the same quality as the thermal model [1, 2] or the relativistic self-consistent chiral model used in [3]. Within the thermal model the particle production fractions are reproduced with a temperature $T = 174 \pm 7$ MeV and a baryonic chemical potential $\mu_B = 46 \pm 5$ MeV, while for the chiral model these quantities are $T = 155$ MeV and the baryon chemical potential of the order of $\mu_B = 51$ MeV. In [4] these numbers lie in the range $146 < T < 153$ MeV and $46.5 < \mu_B < 62.8$ MeV. In [5] the parameters related to the coupling of the hyperons to the mesons were adjusted in accordance with the different hyperonic binding energies and the numbers for

the freeze-out temperature and chemical potential with a modified GM3 [11] parametrization were $T = 147.7$ MeV and $\mu_B = 31.6$ MeV. It is worth mentioning that all those numbers depend on the set of hyperon couplings, a value not well known.

In the present paper we test the behaviour of the quark meson coupling model (QMC) in this regime of temperature and density. Within the QMC model, nuclear matter is described as a system of nonoverlapping MIT bags which interact through the effective scalar and vector mean fields [15]. Although the QMC model shares many similarities with the non-linear Walecka models (NLWM) [8], it also offers new opportunities for studying nuclear matter properties. One of the most attractive aspects of the model is that different phases of hadronic matter, from very low to very high baryon densities and temperatures, can be described within the same underlying model.

In the QMC the internal structure of the nucleon is introduced explicitly and matter at low densities and temperatures is a system of nucleons interacting through meson fields, with quarks and gluons confined within MIT bags. For matter at very high density and/or temperature, one expects that baryons and mesons dissolve and the entire system of quarks and gluons becomes confined within a single, big MIT bag. In most cases in the literature, the energy of the nucleonic MIT bag is identified with the effective mass of the nucleon. This identification has important implications: at finite temperature, while in the NLWM models the nucleon mass always decreases with temperature, in the QMC it increases [16]. The difference arises due to the explicit treatment of the internal structure of the nucleon in the QMC. When the bag is heated up, quark-antiquark pairs are excited in the interior of the bag, increasing the internal energy of the bag. In the present approach, we identify the effective mass of the nucleon with the free energy of the bag, and as it is shown next a direct consequence is the recovery of the behaviour of the NLWM for the effective mass, i.e., it decreases with the increase of the temperature. This choice makes sense because we want to identify the temperature as a state variable. Next we discuss some of the consequences of this choice and apply the QMC to the description of hadron abundances and particle ratios in Au-Au with $s = \sqrt{130}$ GeV collisions at RHIC/BNL and Pb-Pb collisions at SPS.

The paper is organized as follows: in section II we give a brief review of the QMC model and its generalization for finite temperatures; in section III we present some results referring the description of warm nuclear matter within the QMC and apply the formalism to the description of particle production in Au-Au $s = \sqrt{130}$ GeV collisions at RHIC/BNL and Pb-Pb collisions at SPS.; in section IV we draw our final conclusions.

II. FORMALISM

In the QMC model, the nucleon in nuclear medium is assumed to be a static spherical MIT bag in which quarks interact with the scalar and vector fields, σ , δ , ω and ρ and these fields are treated as classical fields in the mean field approximation[15, 16]. The quark field $\psi_q(\mathbf{r}, t)$ inside the bag then satisfies the Dirac equation

$$\left[i\vec{\gamma} \cdot \vec{\partial} - (m_q^0 - V_\sigma) - \gamma^0 (V_\omega + \frac{1}{2}\tau_{3q}V_\rho) \right] \psi_q(\mathbf{r}, t) = 0, \quad (1)$$

with $q = u, d, s$, where $V_\sigma = g_\sigma^q \sigma_0$, $V_\omega = g_\omega^q \omega_0$ and $V_\rho = g_\rho^q \rho_{03}$ with σ_0 , ω_0 and ρ_{03} being the classical meson fields. g_σ^q , g_ω^q and g_ρ^q are the quark meson couplings with the σ , ω and ρ mesons respectively and m_q^0 is the current quark mass. The normalized ground state for a quark in the bag is given by

$$\psi_q(\mathbf{r}, t) = \mathcal{N}_q \exp(-i\epsilon_q t/R_B) \begin{pmatrix} j_0\left(\frac{x_q}{R_B}\right) \\ i\beta_q \vec{\sigma} \cdot \hat{r} j_1\left(\frac{x_q r}{R_B}\right) \end{pmatrix} \frac{\chi_q}{\sqrt{4\pi}}, \quad (2)$$

where

$$\epsilon_q = \Omega_q + R_B \left(g_\omega^q \omega_0 + \frac{1}{2} g_\rho^q \tau_z \rho_{03} \right); \quad (3)$$

$$\beta_q = \sqrt{\frac{\Omega_q - R_B m_q^*}{\Omega_q + R_B m_q^*}},$$

with the normalization factor given by

$$\mathcal{N}_q^{-2} = 2R_B^3 j_0^2(x_q) [\Omega_q(\Omega_q - 1) + R_B m_q^*/2] / x_q^2, \quad (4)$$

where $\Omega_q \equiv \sqrt{x_q^2 + (R_B m_q^*)^2}$, $m_q^* = m_q^0 - g_\sigma^q \sigma_0$, R_B is the bag radius of the baryon B , and χ_q is the quark spinor. The quantities ψ_q , ϵ_q , β_q , \mathcal{N}_q , Ω_q , m_q^* all depend on the baryon considered. The bag eigenvalue, x_q , is determined by the boundary condition at the bag surface

$$j_0(x_q) = \beta_q j_1(x_q). \quad (5)$$

At finite temperatures, the three quarks inside the bag can be thermally excited to higher angular momentum states and also quark-antiquark pairs can be created. For simplicity, we assume that the bag describing the nucleon continues to remain in a spherical shape with radius R , which is now temperature dependent. The single-particle energies in units of R^{-1} are given as

$$\epsilon_q^{n\kappa} = \Omega_q^{n\kappa} + R_B (V_\omega \pm \frac{1}{2} V_\rho), \quad (6)$$

for the quarks and

$$\epsilon_q^{n\kappa} = \Omega_q^{n\kappa} - R_B (V_\omega \pm \frac{1}{2} V_\rho), \quad (7)$$

for the anti-quarks, where the + sign is for u quarks and – for d quarks, and

$$\Omega_q^{n\kappa} = \sqrt{x_{n\kappa}^2 + R_B^2 m_q^{*2}}. \quad (8)$$

The eigenvalues $x_{n\kappa}$ for the state characterized by n and κ are determined by the boundary condition at the bag surface,

$$i\gamma \cdot n \psi_q^{n\kappa} = \psi_q^{n\kappa}. \quad (9)$$

Thus, the quark eigenvalues $x_{n\kappa}$ become modified by the surrounding nucleon medium at finite temperature. The total energy from the quarks and anti-quarks at finite temperature is

$$E_{tot} = \sum_{q,n,\kappa} \frac{\Omega_q^{n\kappa}}{R_B} (f_{n\kappa}^q + f_{n\kappa}^{\bar{q}}), \quad (10)$$

where

$$\begin{aligned} f_{n\kappa}^q &= \frac{1}{e^{(\Omega_q^{n\kappa}/R_B - \nu_q)/T} + 1} \\ f_{n\kappa}^{\bar{q}} &= \frac{1}{e^{(\Omega_q^{n\kappa}/R_B + \nu_q)/T} + 1}, \end{aligned} \quad (11)$$

with ν_q being the effective quark chemical potential, related to the quark chemical potential μ_q as

$$\nu_q = \mu_q - V_\omega - m_\tau^q V_\rho. \quad (12)$$

The energy of a static bag describing baryons consisting of three ground state quarks can be expressed as

$$E_B^{\text{bag}} = E_{tot} - \frac{Z_B}{R_B} + \frac{4}{3} \pi R_B^3 B_B, \quad (13)$$

where Z_B is a parameter which accounts for zero-point motion and B_B is the bag constant. The entropy of the bag is defined as

$$\begin{aligned} \mathcal{S}_B^{\text{bag}} &= - \sum_{q,n,\kappa} \left[f_{n\kappa}^q \ln f_{n\kappa}^q + (1 - f_{n\kappa}^q) \ln(1 - f_{n\kappa}^q) \right. \\ &\quad \left. + f_{n\kappa}^{\bar{q}} \ln f_{n\kappa}^{\bar{q}} + (1 - f_{n\kappa}^{\bar{q}}) \ln(1 - f_{n\kappa}^{\bar{q}}) \right], \end{aligned} \quad (14)$$

and the free energy for the bag is given by

$$F_B^{\text{bag}} = E_B^{\text{bag}} + T \mathcal{S}_B^{\text{bag}} \quad (15)$$

The set of parameters used in the present work is given in Ref. [17]. The effective mass of a nucleon bag at rest is taken to be

$$M_B^* = F_B^{\text{bag}}. \quad (16)$$

In reference [16], it was considered the bag energy instead of the free energy to define the effective mass. The equilibrium condition for the bag is then obtained by

minimizing the effective mass, M_B^* with respect to the bag radius

$$\frac{dM_B^*}{dR_B^*} = 0. \quad (17)$$

Once the bag radius is obtained, the effective baryon mass is immediately determined. For a given temperature T and scalar field σ , the effective quark chemical potentials, ν_q , are determined from the total number of quarks, isospin density and strangeness, i.e.,

$$n_0^j = \sum_{q,n,\kappa} (f_{nq}^q - f_{nq}^{\bar{q}}) \equiv 3, \quad (18)$$

$$n_3^j = \sum_{q,n,\kappa} 2m_{\tau(q)} (f_{nq}^q - f_{nq}^{\bar{q}}) \equiv 2m_{\tau(j)}, \quad (19)$$

$$r_s^j = \sum_{q,n,\kappa} r_s(q) (f_{nq}^q - f_{nq}^{\bar{q}}). \quad (20)$$

In our calculation we consider $j = \Lambda$.

The total energy density of baryonic matter at finite temperature T and at finite baryon density ρ_B is

$$\begin{aligned} \mathcal{E} &= \frac{2}{(2\pi)^3} \sum_{i=B} \int d^3k [\epsilon^* (f_i + \bar{f}_i) + \mathcal{V}_{0i} (f_i - \bar{f}_i)] \\ &\quad + \frac{1}{2} m_\sigma^2 \sigma^2 - \frac{1}{2} m_\omega^2 \omega^2 - \frac{1}{2} m_\rho^2 \rho_{03}^2, \end{aligned} \quad (21)$$

where f_i and \bar{f}_i are the thermal distribution functions for the baryons and anti-baryons,

$$f_B = \frac{1}{e^{(\epsilon^* - \nu_B)/T} + 1} \quad \text{and} \quad \bar{f}_B = \frac{1}{e^{(\epsilon^* + \nu_B)/T} + 1}, \quad (22)$$

$\epsilon^* = (\vec{k}^2 + M_B^{*2})^{1/2}$ the effective nucleon energy, $\nu_B = \mu_B - \mathcal{V}_{0B}$ the effective baryon chemical potential and $\mathcal{V}_{0B} = g_{\omega B} \omega + I_{3B} g_{\rho B} b_{03}$ (I_{3B} is the isospin projection of the baryon species B). The couplings of the mesons with the baryons, $g_{\omega B}$ and $g_{\rho B}$, will be discussed below. The thermodynamic grand potential density and the free energy density are defined as

$$\Omega = \mathcal{F} - \sum_{i=B} \mu_i \rho_i, \quad \mathcal{F} = \mathcal{E} - T\mathcal{S}, \quad (23)$$

with the entropy density $\mathcal{S} = S/V$ given by

$$\begin{aligned} \mathcal{S} &= - \sum_{i=B} \frac{2}{(2\pi)^3} \int d^3k \left[f_i \ln f_i + (1 - f_i) \ln(1 - f_i) \right. \\ &\quad \left. + \bar{f}_i \ln \bar{f}_i + (1 - \bar{f}_i) \ln(1 - \bar{f}_i) \right]. \end{aligned} \quad (24)$$

The baryon density (of each baryon species) is given by

$$\rho_i = \frac{2}{(2\pi)^3} \int d^3k (f_i - \bar{f}_i), \quad (25)$$

so that the total baryon density is $\rho = \sum_{i=B} \rho_i$. The pressure is the negative of Ω , which after an integration

by parts can be written as

$$P = \frac{1}{3} \sum_{i=B} \frac{2}{(2\pi)^3} \int d^3k \frac{\mathbf{k}^2}{\epsilon^*(k)} (f_i + \bar{f}_i) - \frac{1}{2} m_\sigma^2 \sigma^2 + \frac{1}{2} m_\omega^2 \omega^2 + \frac{1}{2} m_\rho^2 \rho_{03}^2. \quad (26)$$

From the above expression the pressure depends explicitly on the meson mean fields σ , ω and ρ_{03} . It also depends on the baryon effective mass M_B^* which in turn also depends on the sigma field (see Eqs. (10-17)). At a given temperature and for given baryon density, the effective mass is known for given values of the meson fields, once the bag radius R_B and the effective quark chemical potentials ν_q are calculated by using Eqs. (18)-(20). The σ meson field is determined through

$$\frac{\partial P}{\partial \sigma} = \left(\frac{\partial P}{\partial M_N^*} \right)_{\mu_i, T} \frac{\partial M_N^*}{\partial \sigma} + \left(\frac{\partial P}{\partial \sigma} \right)_{M_N^*} = 0. \quad (27)$$

$$m_\omega^2 \omega_0 = \sum_{i=B} g_{\omega B} \rho_i, \quad (28)$$

$$m_\rho^2 \rho_{03} = \sum_{i=B} g_{\rho B} I_{3B} \rho_i. \quad (29)$$

The hyperon couplings are not relevant to the ground state properties of nuclear matter, but information about them can be available from the levels in Λ hypernuclei [11, 18, 19]:

$$g_{\sigma B} = x_{\sigma B} g_{\sigma N}, \quad g_{\omega B} = x_{\omega B} g_{\omega N}, \quad g_{\rho B} = x_{\rho B} g_{\rho N}$$

and $x_{\sigma B}$, $x_{\omega B}$ and $x_{\rho B}$ are equal to 1 for the nucleons and acquire different values in different parameterizations for the other baryons. Note that the s -quark is unaffected by the sigma and omega mesons i.e. $g_\sigma^s = g_\omega^s = 0$.

For the bag radius we take $R_N = 0.6$ fm. The two unknowns Z_N and B_N are obtained by fitting the nucleon mass $M = 939$ MeV and enforcing the stability condition for the bag at free space. The values obtained are $Z_N = 3.98699$ and $B_N^{1/4} = 211.303$ MeV for $m_u = m_d = 0$ MeV and $Z_N = 4.00506$ and $B_N^{1/4} = 210.854$ MeV for $m_u = m_d = 5.5$ MeV.

Next we fit the quark-meson coupling constants g_σ^q , $g_\omega = 3g_\omega^q$ and $g_\rho = g_\rho^q$ for the nucleon to obtain the correct saturation properties of the nuclear matter, $E_N \equiv \epsilon/\rho - M = -15.7$ MeV at $\rho = \rho_0 = 0.15$ fm $^{-3}$, $a_{sym} = 32.5$ MeV, $K = 257$ MeV and $M^* = 0.774M$.

Moreover, as we are interested in obtaining also the production of pions and kaons, they are introduced through Bose-Einstein distribution functions

$$\rho_i = \frac{2J_M + 1}{2\pi^2} \int_0^\infty p^2 dp \left[\frac{1}{\exp[(E_i - \mu_i)/T] - 1} \right], \quad (30)$$

TABLE I: Nuclear matter properties.

properties	NL3	TW	QMC
	[9]	[13]	[15]
B/A (MeV)	16.3	16.3	15.7
ρ_0 (fm $^{-3}$)	0.148	0.153	0.150
K (MeV)	271	240	258
\mathcal{E}_{sym} (MeV)	37.4	32.0	32.5
M^*/M	0.60	0.56	0.77

where $i = \pi^+, \pi^-, \pi^0, K^+, K^-, K^0, \bar{K}^0$, and the corresponding vector mesons ρ and K^* , with $J_M = 0$ and 1. $E_i = \sqrt{p^2 + m_i^2}$ and the chemical potentials are again written in terms of their quark constituents, namely, $\mu_{\pi^+} = \mu_u - \mu_d$, $\mu_{K^+} = \mu_u - \mu_s$ and so on. We have considered that they behave like a free gas and their properties are not changed due to their interaction with matter and, therefore, the fraction of produced mesons is determined statistically from their free space properties.

In the sequel we compare the QMC results with the ones obtained within relativistic mean-field models NL3 [9] and TW [13]. For reference we show in Table I the saturation properties of the three models, all very similar.

In order to obtain the particle yields and respective densities three conserved quantities are considered: the total strangeness is set to zero, the total number of baryons and the total isospin are given by $N_B = 2(N + Z) = 394$ and $I_3 = (Z - N)/2 = -39$ in a Au+Au collision and $N_B = 2(N + Z) = 416$ and $I_3 = (Z - N)/2 = -44$ in a Pb-Pb collision. Our code deals with 6 unknowns, the three meson fields and the three independent quark chemical potentials ($\mu_q, q = u, d, s$), solved in a self-consistent manner. We next analyze our results.

III. RESULTS

In Fig.1 the nucleon effective mass is displayed for different temperatures. As mentioned in the Introduction, one can see that the effective mass decreases with the increase of the temperature for a fixed density due to the identification of nucleon effective mass with the free energy of the bag. Up to approximately 50 MeV the the effective mass does not vary much with temperature but around 150 MeV, the temperature of interest for the present study, the decrease with respect to T=0 is huge. This fact has direct consequences in the values of the effective masses obtained for the freeze-out temperature and baryonic densities as is discussed next.

In Fig.2 the nuclear matter free energy is shown for different temperatures and it is seen that it increases considerably. As the free energy of the bag is the main ingredient in the minimization procedure, understanding its behaviour is important.

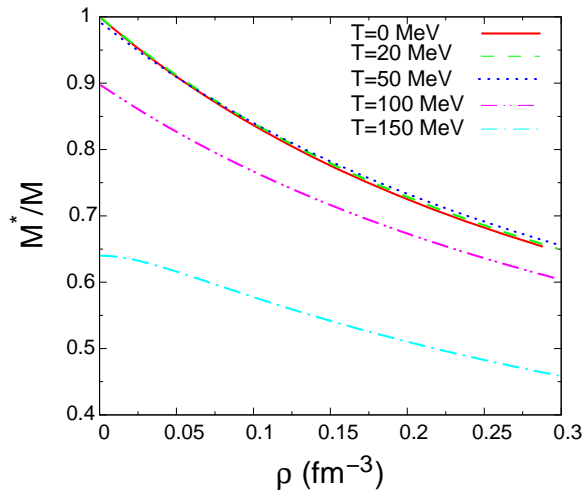


FIG. 1: Effective mass of the nucleon at finite temperature.

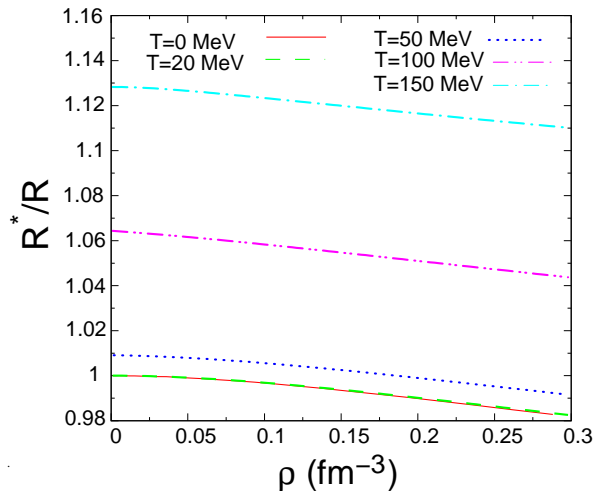


FIG. 3: Radius of the bag at medium at finite temperature.

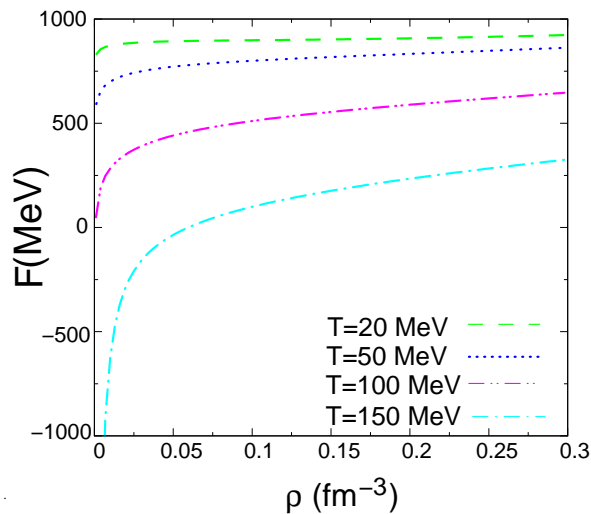


FIG. 2: Free energy of the nuclear matter at finite temperature.

In Fig.3 we show the bag radius for different temperatures and we notice that it swells as the temperature increases. This behaviour is contrary to the one which occurs if the effective mass is identified with the energy of the bag, in which case the bag shrinks with temperature. We expect that the bag swells with temperature and for a high enough temperature the bag should dissolve.

We finally consider the proposed calculation, i.e., the particle yields in heavy ion collisions. For this purpose we have implemented a χ^2 fit as in [1] to obtain the temperature and chemical potential of the freeze-out:

$$\chi^2 = \sum_i \frac{(\mathcal{R}_i^{exp} - \mathcal{R}_i^{theo})^2}{\sigma_i^2}, \quad (31)$$

where \mathcal{R}_i^{exp} and \mathcal{R}_i^{theo} are the i^{th} particle ratio given experimentally and calculated with our models and σ_i represents the errors in the experimental data points. If

the description of the data is consistent the minimum of χ^2 should coincide with the minimum of q^2 defined as

$$q^2 = \sum_i \frac{(\mathcal{R}_i^{exp} - \mathcal{R}_i^{theo})^2}{(\mathcal{R}_i^{theo})^2}. \quad (32)$$

In obtaining the best fit values for the temperature and chemical potentials, we have used the experimental ratios appearing in Table II four times for \bar{p}/p , twice for π^-/π^+ and four times for K^-/K^+ , all with the same weight. We have also taken into account the K^{0*}/h^- and \bar{K}^{0*}/h^- ratios, where h^- is the net sum of all negative electrically charged hadrons. Instead we could have taken the mean value of the measured values and a statistical average value of the errors. In Table II we show the experimentally measured ratios, the QMC results calculated in the present work and the results obtained for the NL3 parametrization [9] and the TW parametrization of a density dependent hadron model [13], given in [4]. In Table III we compare the baryon effective masses obtained within QMC with the ones in NL3 and TW models for the temperature and baryon chemical potential indicated in Table II. In this table N stands for nucleons. It is seen that QMC predicts smaller effective masses than NL3 and TW due to the internal structure of baryons within this model, as discussed earlier. As a consequence in QMC we obtain larger values for the ratios antiparticles/particles, as well as \bar{p}/π^- , when compared with NL3 and TW. Smaller effective masses also allow the reproduction of the experimental ratios with a lower temperature. A lower temperature may explain the smaller kaon yields of QMC with respect to NL3 and TW, and therefore smaller ratios for K^-/π^- , and K^{0*}/h^- , \bar{K}^{0*}/h^- .

Anyhow, as in [4] the effective masses and the value of the fireball temperature seem to show that the freeze out occurs below the critical temperature, at a temperature below the phase transition to a massless baryon phase.

QMC seems to do less well in reproducing the meson yields and this is probably due to the simplified way

TABLE II: Comparison of Au-Au experimental particle ratios (RHIC), relativistic mean field models and quark-meson coupling model results.

ratio	exp. data	exp	NL3	TW	QMC
			[9]	[13]	[15]
\bar{p}/p	0.65±0.07	STAR	0.650	0.656	0.738
	0.64±0.07	PHENIX			
	0.60±0.07	PHOBOS			
	0.64±0.07	BRAHMS			
\bar{p}/π^-	0.08±0.01	STAR	0.075	0.076	0.083
π^-/π^+	1.00±0.02	PHOBOS	0.998	1.01	0.999
	0.95±0.06	BRAHMS			
K^-/K^+	0.88±0.05	STAR	0.912	0.896	1.001
	0.78±0.13	PHENIX			
	0.91±0.09	PHOBOS			
	0.89±0.07	BRAHMS			
K^-/π^-	0.149±0.02	STAR	0.234	0.228	0.191
$\bar{\Lambda}/\Lambda$	0.77±0.07	STAR	0.681	0.663	0.681
$\bar{\Xi}^-/\Xi^-$	0.82±0.08	STAR	0.746	0.739	0.713
K^{0*}/h^-	0.06 ± 0.017	STAR	0.058	0.064	0.037
\bar{K}^{0*}/h^-	0.058 ± 0.017	STAR	0.053	0.056	0.037
Λ/h^-			0.021	0.023	0.023
$T(\text{MeV})$			149	146.6	132
$\mu_b (\text{MeV})$			47.5	62.8	32.5
$\rho \times 10^{-3} (\text{fm}^{-3})$			8.37	4.90	3.08
χ^2			23.94	22.18	27.56
q^2			0.21	0.19	0.80

TABLE III: Effective masses obtained with the temperature and chemical potentials given in Table II.

	NL3	TW	QMC
	[9]	[13]	[15]
M_N^*/M_N	0.88	0.87	0.78
M_Λ^*/M_Λ	0.93	0.92	0.83
M_Σ^*/M_Σ	0.94	0.93	0.84
M_Ξ^*/M_Ξ	0.94	0.93	0.85
$M_{\Sigma^*}^*/M_{\Sigma^*}$	0.95	0.94	0.84
$M_{\Xi^*}^*/M_{\Xi^*}$	0.94	0.94	0.72

mesons have been included in the present calculation, just as free particles. Interactions would certainly affect their effective masses and a better fit could probably be obtained as discussed in [5]. In fact the mesons could also have been described as bags like in [20].

Next we describe within QMC the Pb-Pb experimental particle ratios obtained at SPS supposing that chemical equilibrium was attained before freeze-out. The authors of [21] have shown within an improved statistical

model with excluded volume and resonance decays, that the experimental hadronic yields and their ratios at SPS energy are compatible with a chemical equilibrium population. From the whole set of existing experimental data we have chosen all ratios involving the baryonic octet, pions and charged kaons. For the antiproton/proton ratio we took only the ones excluding feeding from weak decays. Within QMC we were not able to fit the data with a χ^2 lower than 216 and $q^2 = 17.3$. The results are given in Table IV, where the ratios obtained with NL3 are also shown. For NL3 the minimum χ^2 is smaller but with a huge q^2 . In the last column we give the NL3 results for $q^2 = 17.3$ (NL3'), the value obtained with QMC. For the new fit the ratios get closer to the experimental data but the anti-particles and hyperons are still badly described.

We have not considered either heavier-resonance decays neither feeding from weak decays as done in [21]. Weak decay affects mainly the ratios involving Ξ . If these ratios are calculated as half the original ratio, for the NL3 model (shown in Table IV as NL3*), the χ^2 value improves considerably. But this is not the case when the QMC model is employed. It is important to mention that the best fit obtained for the SPS data in [21] gave $T = 168 \pm 2.4$ and $\mu_b = 266 \pm 5$, both values much higher than ours. In [21], $\chi^2 = 37.8$ was also far away from the ideal value.

IV. CONCLUSIONS

In the present work we have described the particle yield ratios in Au+Au at RHIC and in Pb+Pb at SPS assuming thermal and chemical equilibrium within the QMC model, to test this model in the high temperature and low density regime. Within the QMC model, nuclear matter is described as a system of non-overlapping MIT bags which interact through the effective scalar and vector mean fields [15]. We have identified the free energy of the baryonic MIT bag with the effective mass of each baryon and verified that, at finite temperature, the effective mass of the nucleons decreases with temperature and that a swelling of the MIT bag occurs. In previous studies the energy of the MIT bag had been identified with the effective mass and, at finite temperature, this gave rise to an increase of the effective nucleonic mass with temperature, contrary to what occurs in other relativistic mean-field nuclear models, and a resulting decrease of the bag radius with temperature.

We have applied the QMC model to the description of the particle yield ratios in Au+Au at RHIC with success for a temperature of 132 MeV and a baryonic chemical potential of 32.5 MeV. These values are lower than the values obtained within a description using NLWM or density dependent hadronic models [4] because QMC predicts a faster reduction of the effective masses with temperature and therefore, for a given temperature, a larger anti-particle production. An improvement of the present calculation would also take into account the bag

TABLE IV: Comparison of Pb-Pb experimental particle ratios (SPS), and quark-meson coupling model results. NL3* refers to a fit supposing that 50% of the Ξ yield decays. NL3' corresponds to the fit with $q^2 = 17.3$, the value obtained with QMC.

ratio	exp. data	exp	QMC	NL3	NL3*	NL3'
			[15]			
$(p - \bar{p})/h^-$	0.228 ± 0.029	NA49	0.213	0.244	0.256	0.207
\bar{p}/p	0.055 ± 0.01	NA44	0.095	0.0003	0.079	0.003
Λ/h^-	0.077 ± 0.011	WA97	0.007	0.00002	0.008	0.002
π^-/π^+	1.1 ± 0.1	NA49	0.997	1.066	1.101	1.072
K^+/K^-	1.85 ± 0.09	NA44	1.001	1.854	1.824	1.656
	1.8 ± 0.1	NA49				
$\bar{\Lambda}/\Lambda$	0.131 ± 0.017	WA97	0.087	0.0006	0.099	0.043
Ξ^-/Λ	0.11 ± 0.01	WA97	0.117	0.120	0.128	0.23
$\Xi^+/\bar{\Lambda}$	0.188 ± 0.039	NA49	0.122	0.222	0.233	0.380
	0.206 ± 0.04	WA97				
$(\Xi^+ + \Xi^-)/(\bar{\Lambda} + \Lambda)$	0.13 ± 0.03	NA49	0.117	0.120	0.138	0.237
Ξ^+/Ξ^-	0.232 ± 0.033	NA49	0.091	0.001	0.181	0.071
	0.247 ± 0.043	WA97				
$T(\text{MeV})$			130	99	156.1	140.
$\mu_b (\text{MeV})$			167.5	411	330.2	303.
$\rho \times 10^{-3} (\text{fm}^{-3})$			0.019	0.007	0.064	0.030
χ^2			216	186	20.07	285
q^2			17.32	1.7×10^5	0.48	17.31

structure of the pions and kaons. As a consequence the effective mass of these mesons would change with temperature contrary to what has been considered in the present calculation.

We have also applied the QMC to the description of the particle production ratios in Pb+Pb in SPS. If the data are taken without the assumption of weak decays, the description of the experimental yield ratio is not very good within the NL3 model, but improves when this assumption is considered. Within the QMC models the

results are always poor.

ACKNOWLEDGMENTS

This work was partially supported by CNPq(Brazil), the FCT/CAPES-2009 collaboration and by FEDER/FCT (Portugal) under the projects CERN/FP/83505/2008 and PTDC/FIS/64707/2006.

-
- [1] P. Braun-Munzinger, I. Heppe and J. Stachel, Phys. Lett. **B 465**, 15 (1999).
- [2] P. Braun-Munzinger, D. Magestro, K. Redlich and J. Stachel, Phys. Lett. **B 518**, 41 (2001).
- [3] D. Zschesche, S. Schramm, J. Schaffner-Bielich, H. Stöcker and W. Greiner, Phys. Lett. **B 547**, 7 (2002).
- [4] D.P. Menezes, C. Providência, M. Chiapparini, M. E. Bracco, A. Delfino, and M. Malheiro, Phys. Rev. **C76** (2007) 064902.
- [5] M. Chiapparini, M. E. Bracco, A. Delfino, M. Malheiro, D.P. Menezes and C. Providência, Nucl. Phys. **A**, submitted o publication.
- [6] NA49 Collaboration, H. Appelshäuser et al., Phys. Lett. **B 444**, 523 (1998); F. Gabler, J. Phys. **G 25**, 199 (1999) and many others.
- [7] WA Collaboration, E. Andersen et al., J. Phys. **G 25**, 171 (1999); E. Andersen et al., Phys. Lett. **B 449**, 401 (1999) and many others.
- [8] B. Serot and J.D. Walecka, *Advances in Nuclear Physics* 16, Plenum-Press, (1986) 1.
- [9] G. A. Lalazissis, J. König and P. Ring, Phys. Rev. C **55**, 540 (1997).
- [10] K. Sumiyoshi, H. Kuwabara, H. Toki, Nucl. Phys. **A 581**, 725 (1995).
- [11] N. K. Glendenning, Compact Stars, Springer-Verlag, New-York, 2000.
- [12] C.J. Horowitz and J.Piekarewicz, Phys. Rev. **C 64**, 062802R (2001); J.K. Bunta and S. Gmuca, Phys. Rev. C **68**, 054318 (2003); J.K. Bunta and S. Gmuca, Phys. Rev. C **70**, 054309 (2004).
- [13] S. Typel and H. H. Wolter, Nucl. Phys. **A656**, 331 (1999).
- [14] T. Niksic, D. Vretenar, P. Finelli and P. Ring, Phys. Rev. **C 66**, 024306 (2002); D. Vretenar, T. Niksic and P. Ring,

- Phys. Rev. C **68**, 024310 (2003).
- [15] P. A. M. Guichon, Phys. Lett. **B 200**, 235 (1988); K. Saito and A.W. Thomas, Phys. Lett. **B 327**, 9 (1994); K. Tsushima, K. Saito, A.W. Thomas and S.V. Wright, Phys. Lett. **B 429**, 239 (1998).
- [16] P.K. Panda, A. Mishra, J.M. Eisenberg, W. Greiner, Phys. Rev. C **56**, 3134 (1997); P.K. Panda, G. Krein, D.P. Menezes and C. Providencia, Phys. Rev. C **68**, 015201 (2003).
- [17] P.K. Panda, D.P. Menezes and C. Providencia, Phys. Rev. C **69**, 025207 (2004).
- [18] R.E. Chrien and C.B. Dover, Annu. Rev. Nucl. Part. Sci. **39**, 113 (1989).
- [19] S.A. Moszkowski, Phys. Rev. D **9**, 1613 (1974).
- [20] K. Tsushima, K. Saito, A. W. Thomas, and S. V. Wright, Phys. Lett. **B 429**, 239 (1998); D. P. Menezes, P. K. Panda, and C. Providencia, Phys. Rev. C **72**, 035802 (2005).
- [21] P. Braun-Munzinger, I. Heppe, J. Stachel, Phys. Lett. **B 465**, 15 (1999).